

HERMETIC PACKAGES AND FEEDTHROUGHS FOR NEURAL PROSTHESES

Quarterly Progress Report # 3

(Contract NIH-NINCDS-N01-NS-4-2319)

(Contractor: The Regents of the University of Michigan)

For the Period:

April-June 1995

Submitted to the

*Neural Prosthesis Program
National Institute of Neurological Disorders and Stroke
National Institutes of Health*

By the

*Center For Integrated Sensors and Circuits
Department of Electrical Engineering and Computer Science
University of Michigan
Ann Arbor, Michigan 48109-2122*

Program Personnel:

UNIVERSITY OF MICHIGAN

Professor Khalil Najafi: Principal Investigator

Graduate Student Research Assistants:

Mr. Anthony Coghlan: RF Telemetry & Microstimulator Assembly

Mr. Mehmet Dokmeci: Packaging and Accelerated Testing

Mr. Mark Nardin: Microstimulator Circuit Design/Fabrication

Mr. Jeffrey Von Arx: Electrode and Package Fabrication/Testing

VANDERBILT UNIVERSITY

Professor David L. Zeale, Principal Investigator

July 1995

SUMMARY

During the past quarter we achieved major progress in several areas, including the continued testing of our glass packages under accelerated conditions, in-vivo animal testing of the old glass packages at Vanderbilt, initial testing of the new glass packages and package substrates, and assembly and packaging of complete microstimulators.

Our most significant package testing results to date are those obtained from a series of silicon-glass packages that have been soaking in DI water at 85°C and 95°C for the past several months. We have one package that has lasted for more than 318 days at 95°C, and four that have lasted more than 321 days at 85°C in DI water. During the last quarter we lost one of the packages that was soaking at 95°C, so there are now one package at 95°C and four at 85°C still under test without any sign of leakage in them. Calculation of MTTF for these glass packages using the data obtained so far indicates a worst-case lifetime of about 8 years, and a best-case lifetime of about 60 years at body temperatures. Both of these numbers are very good given the fact that these accelerated tests are still ongoing. We also have 5 packages soaking at room temperature in saline for over 222 days, and these have not shown any sign of leakage either.

Several glass packages were implanted and tested in rats at Vanderbilt University. The packages were implanted in the dorsum of rats. After 1 month, the device and surrounding tissue were harvested from these rats. Histology tests on the recovered tissue did not show any sign of rejection. There was no evidence of edema or inflammatory reaction. These results, although obtained from rather short-term experiments, are very encouraging because they clearly indicate that there are no adverse effects on the tissue from the materials used in the microstimulator. We will obviously continue these tests aiming at more chronic experiments in the future.

A new set of ceramic capacitors have been acquired that can withstand the high temperature environment during electrostatic bonding. The characteristics of these capacitors have been fully tested to temperatures as high as 400°C, and change very slightly. These capacitors will be used in the single-channel microstimulators.

We have bonded a number of the new ultrasonically machined glass capsules to new silicon package substrates and have been able to achieve excellent bond quality to full-thickness silicon substrates. This is a very significant result because it eliminates the need for thinning the silicon substrate. The bond quality is very good. Initial soak tests have begun on these packages and indicate a hermetic seal. Additional packages are being fabricated and more soak tests will be under way using these new glass capsules.

During the past quarter we also developed the procedures for the complete assembly and packaging of all the components of the single-channel microstimulator. Several issues dealing with the attachment of the microcoil and the chip capacitor have been resolved. The microcoils are attached using a microwelder to copper-plated bonding pads on the circuit chip, while the capacitor is attached to the same chip using conductive epoxy. We also developed the process for forming the copper coils on the receiver circuit chip. A layer of low-temperature oxide is used to passivate the first metal layer which interconnects the circuitry. This process is now very simple and has been performed on a number of wafers. First-generation and second-generation chips from these wafers are now under test.

These chips will be used in the coming quarter for the assembly of complete single-channel microstimulators.

1. INTRODUCTION

This project deals with the development of hermetic, biocompatible micropackages and feedthroughs for use in a variety of implantable neural prostheses for sensory and motor handicapped individuals. The project also aims at continuing work on the development of a telemetrically powered and controlled neuromuscular microstimulator for functional electrical stimulation. The primary objectives of the project are: 1) the development and characterization of hermetic packages for miniature, silicon-based, implantable three-dimensional structures designed to interface with the nervous system for periods of up to 40 years; 2) the development of techniques for providing multiple sealed feedthroughs for the hermetic package; 3) the development of custom-designed packages and systems used in chronic stimulation or recording in the central or peripheral nervous systems in collaboration and cooperation with groups actively involved in developing such systems; and 4) establishing the functionality and biocompatibility of these custom-designed packages in *in-vivo* applications. Although the project is focused on the development of the packages and feedthroughs, it also aims at the development of inductively powered systems that can be used in many implantable recording/stimulation devices in general, and of multichannel microstimulators for functional neuromuscular stimulation in particular.

Our group here at the Center for Integrated Sensors and Circuits at the University of Michigan has been involved in the development of silicon-based multichannel recording and stimulating microprobes for use in the central and peripheral nervous systems. More specifically, during the past two contract periods dealing with the development of a single-channel inductively powered microstimulator, our research and development program has made considerable progress in a number of areas related to the above goals. A hermetic packaging technique based on electrostatic bonding of a custom-made glass capsule and a supporting silicon substrate has been developed and has been shown to be hermetic for a period of at least a few years in salt water environments. This technique allows the transfer of multiple interconnect leads between electronic circuitry and hybrid components located in the sealed interior of the capsule and electrodes located outside of the capsule. The glass capsule can be fabricated using a variety of materials and can be made to have arbitrary dimensions as small as 1.8mm in diameter. A multiple sealed feedthrough technology has been developed that allows the transfer of electrical signals through polysilicon conductor lines located on a silicon support substrate. Many feedthroughs can be fabricated in a small area. The packaging and feedthrough techniques utilize biocompatible materials and can be integrated with a variety of micromachined silicon structures.

The general requirements of the hermetic packages and feedthroughs to be developed under this project are summarized in Table 1. Under this project we will concentrate our efforts to satisfy these requirements and to achieve the goals outlined above. There are a variety of neural prostheses used in different applications, each having different requirements for the package, the feedthroughs, and the particular system application. The overall goal of the program is to develop a miniature hermetic package that can seal a variety of electronic components such as capacitors and coils, and integrated circuits and sensors (in particular electrodes) used in neural prostheses. Although the applications are different, it is possible to identify a number of common requirements in all of these applications in addition to those requirements listed in Table 1. The packaging and feedthrough technology should be capable of:

- 1- protecting non-planar electronic components such as capacitors and coils, which typically have large dimensions of about a few millimeters, without damaging them;
- 2- protecting circuit chips that are either integrated monolithically or attached in a hybrid fashion with the substrate that supports the sensors used in the implant;
- 3- interfacing with structures that contain either thin-film silicon microelectrodes or conventional microelectrodes that are attached to the structure;

Table 1: General Requirements for Miniature Hermetic Packages and Feedthroughs for Neural Prostheses Applications

Package Lifetime:

≥ 40 Years in Biological Environments @ 37°C

Packaging Temperature:

≤360°C

Package Volume:

10-100 cc

Package Material:

Biocompatible

Transparent to Light

Transparent to RF Signals

Package Technology:

Batch Manufactureable

Package Testability:

Capable of Remote Monitoring

In-Situ Sensors (Humidity & Others)

Feedthroughs:

At Least 12 with ≤125μm Pitch

Compatible with Integrated or Hybrid Microelectrodes

Sealed Against Leakage

Testing Protocols:

In-Vitro Under Accelerated Conditions

In-Vivo in Chronic Recording/Stimulation Applications

We have identified two general categories of packages that need to be developed for implantable neural prostheses. The first deals with those systems that contain large components like capacitors, coils, and perhaps hybrid integrated circuit chips. The second deals with those systems that contain only integrated circuit chips that are either integrated in the substrate or are attached in a hybrid fashion to the system.

Figure 1 shows our general proposed approach for the package required in the first category. This figure shows top and cross-sectional views of our proposed approach here. The package is a glass capsule that is electrostatically sealed to a support silicon substrate. Inside the glass capsule are housed all of the necessary components for the system. The electronic circuitry needed for any analog or digital circuit functions is either fabricated on a separate circuit chip that is hybrid mounted on the silicon substrate and electrically connected to the silicon substrate, or integrated monolithically in the support silicon substrate itself. The attachment of the hybrid IC chip to the silicon substrate can be performed using a number of different technologies such as simple wire bonding between pads located on each substrate, or using more sophisticated techniques such as flip-chip solder reflow or tab bonding. The larger capacitor or microcoil components are mounted on either the substrate or the IC chip using appropriate epoxies or solders. This completes the assembly of the electronic components of the system and it should be possible to test the system electronically at this point before the package is completed. After testing, the system is packaged by placing the glass capsule over the entire system and bonding it to the silicon substrate using an electrostatic sealing process. The cavity inside the glass package is now hermetically sealed against the outside environment. Feedthroughs to the outside world are provided using the grid-feedthrough technique discussed in previous reports. These feedthroughs transfer the electrical signals between the electronics inside the package and various elements outside of the package. If the package has to interface with conventional microelectrodes, these microelectrodes can be attached to bonding pads located outside of the package; the bond junctions will have to be protected from the external environment using various polymeric encapsulants. If the package has to interface with on-chip electrodes, it can do so by integrating the electrode on the silicon support substrate. Interconnection is simply achieved using on-chip polysilicon conductors that make the feedthroughs themselves. If the package has to interface with remotely located recording or stimulating electrodes that are attached to the package using a silicon ribbon cable, it can do so by integrating the cable and the electrodes again with the silicon support substrate that houses the package and the electronic components within it.

Figure 2 shows our proposed approach to package development for the second category of applications. In these applications, there are no large components such as capacitors and coils. The only component that needs to be hermetically protected is the electronic circuitry. This circuitry is either monolithically fabricated in the silicon substrate that supports the electrodes (similar to the active multichannel probes being developed by the Michigan group), or is hybrid attached to the silicon substrate that supports the electrodes (like the passive probes being developed by the Michigan group). In both of these cases the package is again another glass capsule that is electrostatically sealed to the silicon substrate. Notice that in this case, the glass package need not be a high profile capsule, but rather it need only have a cavity that is deep enough to allow for the silicon chip to reside within it. Note that although the silicon IC chip is originally 500 μm thick, it can be thinned down to about 100 μm , or can be recessed in a cavity created in the silicon substrate itself. In either case, the recess in the glass is less than 100 μm deep (as opposed to several millimeters for the glass capsule). Such a glass package can be easily fabricated in a batch process from a larger glass wafer.

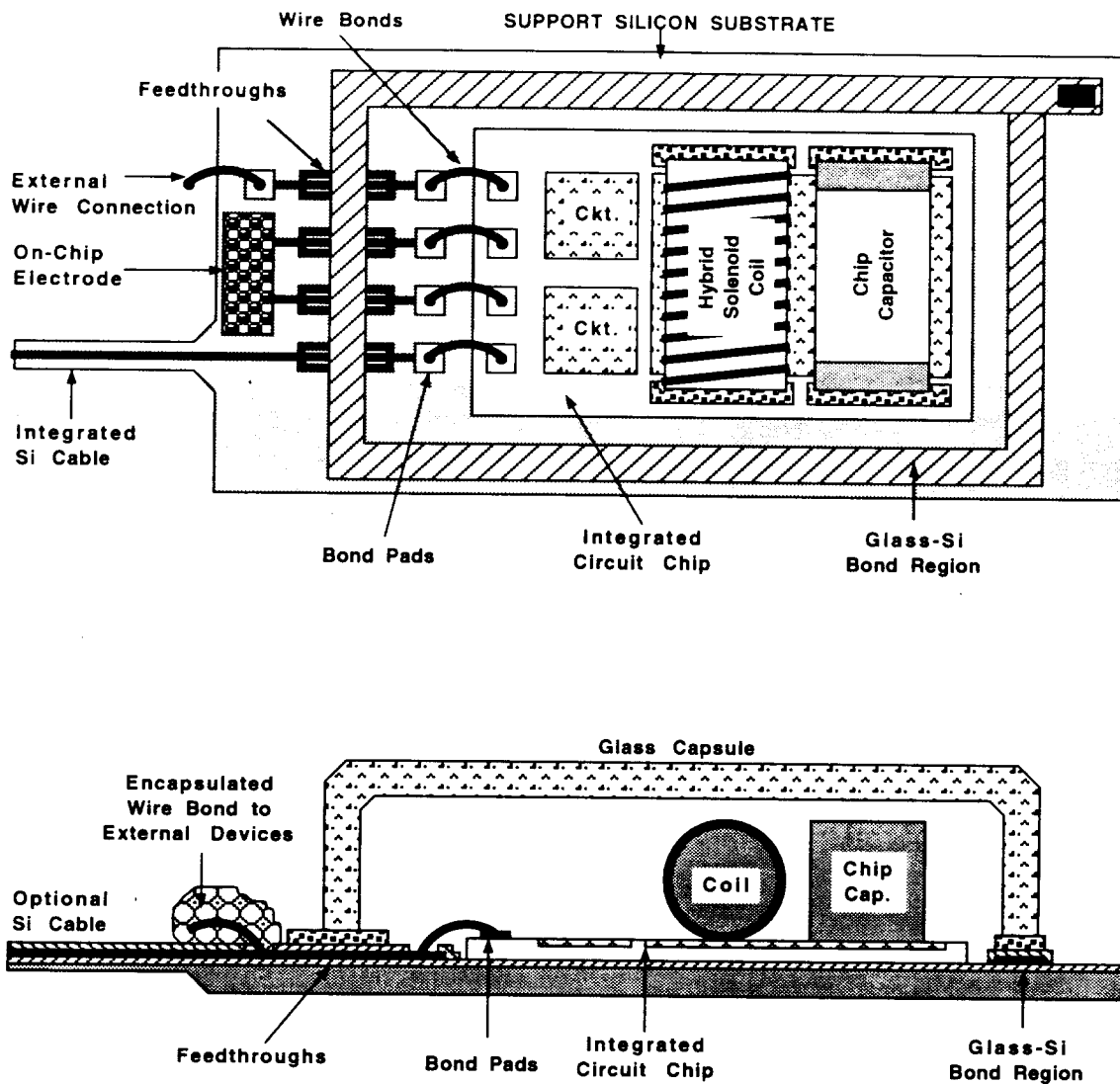


Figure 1: A generic approach for packaging implantable neural prostheses that contain a variety of components such as chip capacitors, microcoils, and integrated circuit chips. This packaging approach allows for connecting to a variety of electrodes.

We believe the above two approaches address the needs for most implantable neural prostheses. Note that both of these techniques utilize a silicon substrate as the supporting base, and are not directly applicable to structures that use other materials such as ceramics or metals. Although this may seem a limitation at first, we believe that the use of silicon is, in fact, an advantage because it provides several benefits. First, it is biocompatible and has been used extensively in biological applications. Second, there is a great deal of effort in the IC industry in the development of multi-chip modules (MCMs), and many of these efforts use silicon supports because of the ability to form high density interconnections on silicon using standard IC fabrication techniques. Third, many present and future implantable probes are based on silicon micromachining technology; the use of our proposed packaging technology is inherently compatible with most of these probes, which simplifies the overall structure and reduces its size.

Once the above packages are developed, we will test them in biological environments by designing packages for specific applications. One of these applications is in recording neural activity from cortex using silicon microprobes developed by the Michigan group under separate contracts. The other involves the chronic stimulation of muscular tissue using a multichannel microstimulator for the stimulation of the paralyzed larynx. This application has been developed at Vanderbilt University. Once the device is built, it will be used by our colleagues at Vanderbilt to perform both biocompatibility tests and functional tests to determine package integrity and suitability and device functionality for the reanimation of the paralyzed larynx. The details of this application will be discussed in future progress reports.

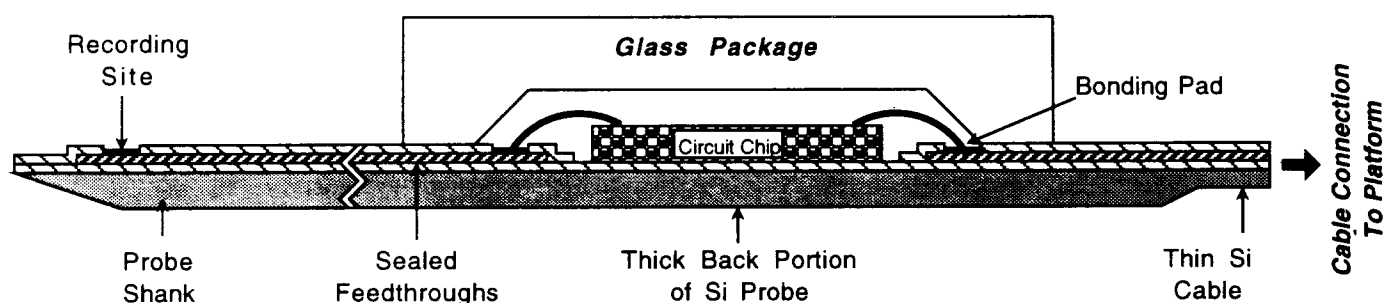


Figure 2: Proposed packaging approach for implantable neural prostheses that contain electronic circuitry, either monolithically fabricated in the probe substrate or hybrid attached to the silicon substrate containing microelectrodes.

2. ACTIVITIES DURING THE PAST QUARTER

2.1 Hermetic Packaging

As has been reported in previous progress reports, we have developed a bio-compatible hermetic package with high density, multiple feedthroughs. This package utilizes electrostatic bonding of a custom-made glass capsule to a silicon substrate to form a hermetically sealed cavity, as shown in Figure 3. Feedthrough lines are obtained by forming closely spaced polysilicon lines and planarizing them with LTO and PSG. The PSG is reflowed at 1100°C for 2 hours to form a planarized surface. A passivation layer of oxide/nitride/oxide is then deposited on top to prevent direct exposure of PSG to moisture. A layer of fine-grain polysilicon (surface roughness <40Å rms) is deposited and doped to act as the bonding surface. Finally, a glass capsule is bonded to this top polysilicon layer by applying a voltage of 2000V between the two for 10 minutes at 320 to 340° C, a temperature compatible with most hybrid components. The glass capsule can be either custom molded from Corning code #7740 glass, or can be batch fabricated using ultrasonic micromachining of #7740 glass wafers.

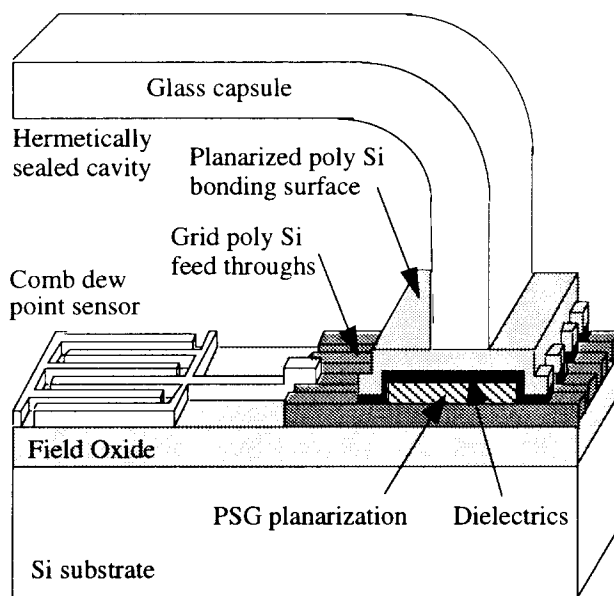


Figure 3: Structure of the hermetic package with grid feedthroughs.

During the past year we have electrostatically bonded and soak tested over one hundred of these packages. The packages successfully prevent leakage in soak tests at 95°C for over 3 months and at 85°C for over 5 months on average. The bonding yield has consistently been 85% (yield is defined as the percentage of packages which last more than 24 hours soaking in DI water), and preliminary in-vivo tests indicate that the package is bio-compatible and rugged.

In the following we will present the progress achieved during the last quarter in the design and testing of the package and in testing of the hybrid components that are eventually housed inside the package.

2.1.1 Improved Packaging Design

As we have mentioned in our previous reports, ultrasonically machined glass capsules have a number of advantages over either molded or hand formed glass capsules, including the fact that they are less expensive, and can be polished to more exacting specifications. As reported previously, an external vendor has manufactured for us hundreds of ultrasonically machined glass capsules (which are formed on 4" glass wafers), and a SEM of one of these new glass capsules is shown in Figure 4. Last quarter we designed a new packaging substrate to match the dimensions and shape of the ultrasonically machined glass capsules. This quarter the substrates were fabricated, electrostatically bonded to silicon substrates, and subjected to long term soak tests.

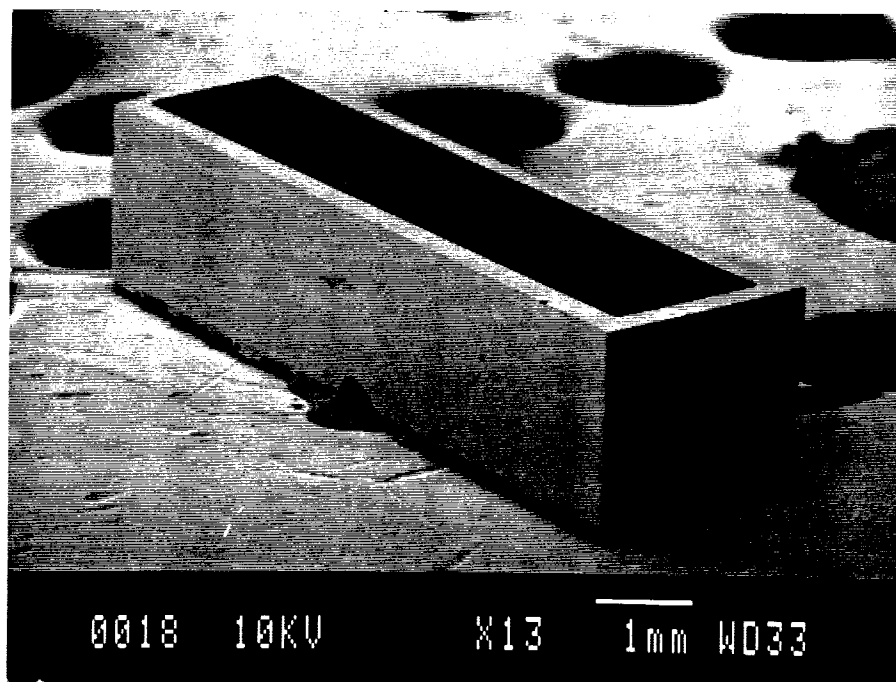


Figure 4: SEM photograph of a new, ultrasonically machined glass capsule.

Twenty wafers with just over 70 packaging substrates on each were fabricated this quarter. Our preliminary soak test results indicate that these new substrates and ultrasonically machined glass capsules provide an excellent seal. Figure 5 shows SEM views of the bonding surface of these new wafers. Although the bonding surface looks very good, upon closer examination one can see very small dimples, and some roughness on the fine-grain polysilicon. The small dimples are created because of the rounded sidewalls of the dry-etched polysilicon lines. The rounded sidewalls are the result of drifting of the optimal etch parameters of the reactive ion etcher (RIE). The RIE etch recipes are now being modified and updated to improve the etch anisotropy for the future runs of the package substrate. The roughness of the polysilicon may be from the additional doping that we perform to reduce the sheet resistance. It is not certain that this doping step is now needed with the new glass capsules and the new substrates. We will perform experiments to determine whether we can improve the surface quality of the polysilicon further. In spite of these two minor problems, we believe that the bonding region is suitable for obtaining a good seal to the glass packages, and we have started soak tests using these substrates. The results of these soak tests will be presented in a later section. We will begin a new fabrication run this quarter to obtain substrates with perfect planarization and polysilicon surface quality.

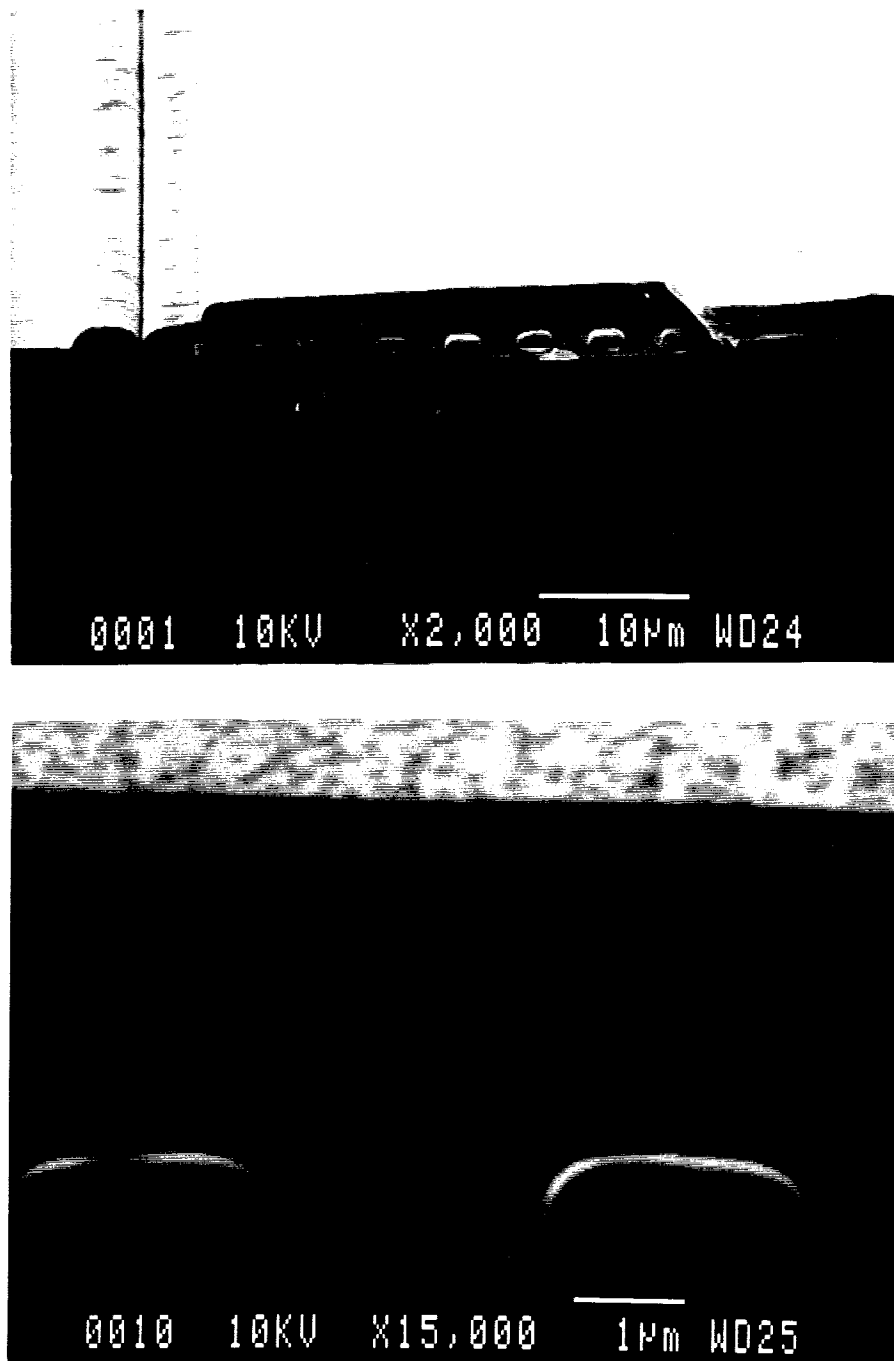


Figure 5: SEM cross-sectional views of the planarized bonding surface of the package substrate.

2.1.2 Characterization of PSG Reflow Time for Planarization

Planarization of the bonding surface is vital to a hermetic seal. Any non-uniformity of more than a few tens of angstroms can be a source of leakage for the package. In order to obtain this level of planarity we have used closely spaced ($2\mu\text{m}$ spacing), narrow ($3\mu\text{m}$ wide) grids of polysilicon for feedthrough lines. These lines are planarized with 1.8 to $2\mu\text{m}$ of PSG deposited on top. This PSG is reflowed at 1100°C for two hours in steam to obtain the near perfect planar surface shown previously. The two hour reflow time was originally chosen based on data extracted from the literature. Cross-sectional SEM's and examination under an atomic force microscope verified that this resulted in a planar surface, but up until this time no effort has been made to see if shorter reflow times can be used. Although for the present microstimulator package a 2 hour, 1100°C reflow step does not cause any problems, it might present difficulties in a variation on this package with a more critical thermal budget. Some examples are: 1) a package with integrated silicon ribbon cables (2 hour, 1100°C reflow will cause shallow boron diffusion to diffuse deeper than desired); and 2) a package that has active circuitry integrated directly onto the packaging substrate. Since the packaging technique we have developed may be used with a wide variety of implantable devices, some of which will probably have critical thermal budgets, the minimum reflow time required for planarization was further examined and characterized.

Figure 6 shows a cross-sectional SEM view of the grid feedthrough lines immediately after PSG deposition, but before reflow. Notice that the PSG is deposited conformally over the feedthrough lines, but that there are still keyhole shaped slots in between the feedthrough lines which are the result of the oxide CVD deposition process. Figure 7 shows a cross-section of the same region after half hour of reflow in steam at 1100°C . Notice that the PSG from nearby the keyhole slots has flown into the slots, thus filling them. This results in a sinusoidal surface pattern with a peak to peak surface roughness of about $0.6\mu\text{m}$. Figure 8 shows the cross-section after 1 hour of reflow. The sinusoidal pattern has smoothed but it is still there, with a peak to peak surface roughness of about $0.3\mu\text{m}$. Finally, Figure 9 shows the surface after 2 hours of reflow. Near perfect planarity has been obtained.

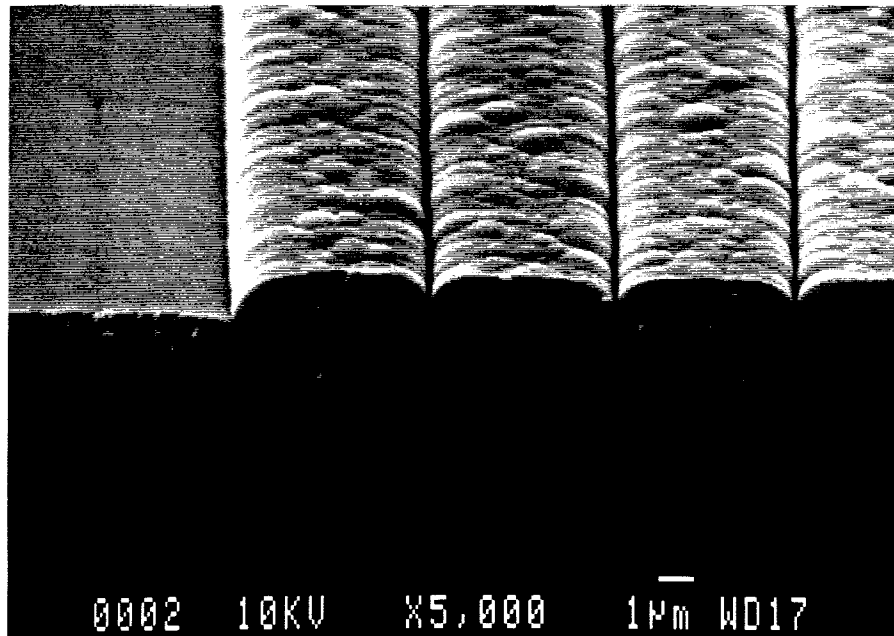


Figure 6: Cross-sectional SEM showing the polysilicon grid feedthrough lines immediately after PSG deposition and before any reflow. Keyhole shaped slots can be seen in the surface.

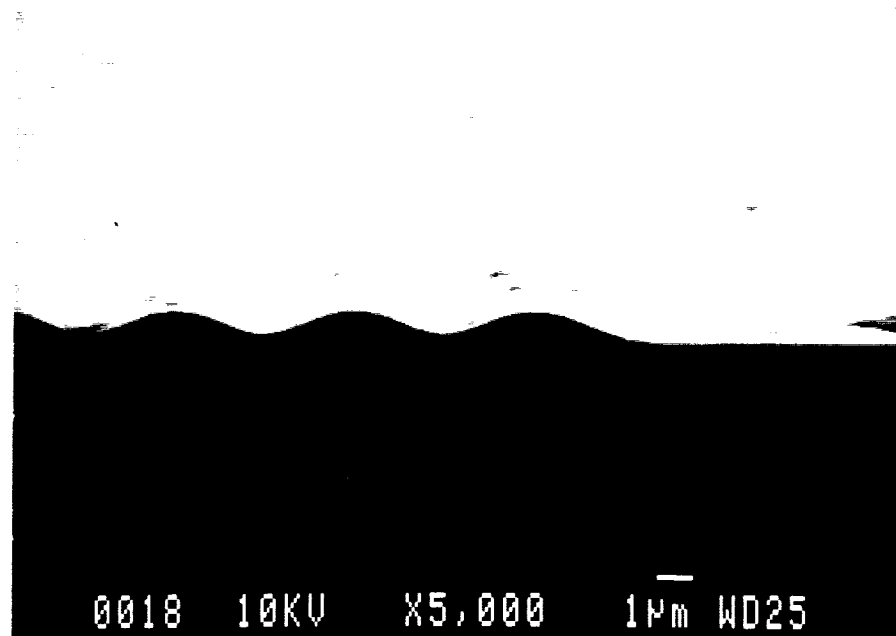


Figure 7: A cross-sectional SEM showing the polysilicon grid feedthrough lines after 1/2 hour of PSG reflow. The surface has a sinusoidal pattern.

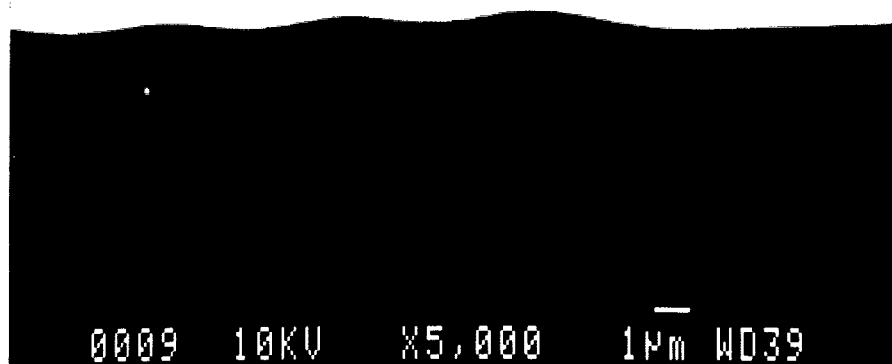


Figure 8: A cross-sectional SEM showing the polysilicon grid feedthrough lines with PSG after 1 hour of reflow. The surface still has a sinusoidal pattern, although as expected, it is much smoother than after 1/2 hour of reflow.

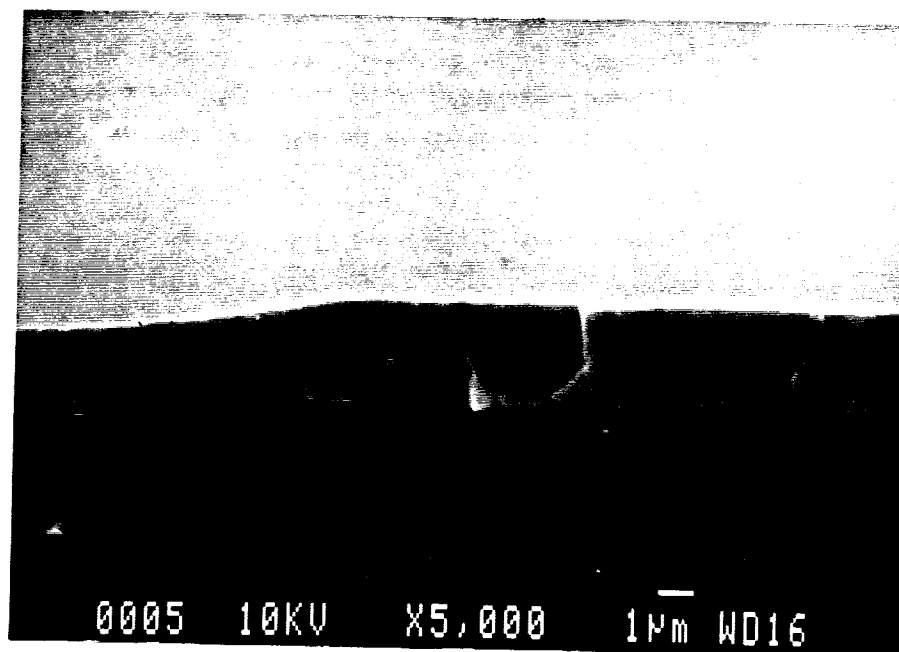


Figure 9: A cross-sectional SEM showing the polysilicon grid feedthrough lines after 2 hours of PSG reflow. The surface is now planar.

The experiments with different reflow times indicate that it is not possible to significantly shorten the reflow time without sacrificing surface planarity. This may cause difficulty in integrating silicon ribbon cables with the package substrates, and we will have to account for this additional thermal budget in order to obtain thin silicon substrates ($\sim 3\mu\text{m}$) to achieve sufficient flexibility. In future quarters we will fabricate substrates with integrated cables for in-vivo hermeticity testing.

2.1.3 Ongoing Accelerated Soak Tests

We have continued accelerated soak testing of the package this past quarter. We had started soaking 10 samples each at 95°C and 85°C in this series of tests. Tables 2 and 3 list some pertinent data for these soak tests. Figure 10 summarizes the results so far from the 95°C soak tests and Figure 11 summarizes the results from the 85°C tests. These figures also list the causes of failure for individual packages when it is known, and they show a curve fit to the lifetime data to illustrate the general trend. The curve fit, however, only approximates the actual package lifetimes since many of the packages failed due to breaking during testing rather than due to leakage.

One of the two remaining packages in the 95°C soak test showed leakage this quarter. Therefore, of the original 10 packages in this test only one package remains after 318 days. None of the packages being soaked at 85°C showed any sign of leakage this quarter, leaving four of the original 10 packages soaking at 85°C after approximately 320 days of testing. Although the number of samples in both of these tests is limited, we believe that the data obtained so far is very encouraging, and we are now beginning to see that the packages soaking at 85°C are demonstrating longer MTTF's than those soaking at 95°C . Although it is early to use the average lifetime obtained from these tests to estimate a MTTF at 37°C , it is still useful to estimate this MTTF using the existing data to see if the data indicates a correct trend.

Table 2: Key data for 95°C soak tests in DI water.

| | |
|--|----------|
| Number of packages in this study | 10 |
| Failed within 24 hours (not included in MTTF) | 1 |
| Packages lost due to mishandling | 2 |
| Longest lasting packages so far in this study | 318 days |
| Packages still under tests with no measurable room temperature condensation inside | 1 |
| Average lifetime to date (MTTF) including losses attributed to mishandling | 100 days |
| Average lifetime to date (MTTF) not including losses attributed to mishandling | 112 days |

Table 3: Key data for 85°C soak tests in DI water.

| | |
|--|----------|
| Number of packages in this study | 10 |
| Failed within 24 hours (not included in MTTF) | 2 |
| Packages lost due to mishandling | 3 |
| Longest lasting packages so far in this study | 321 days |
| Packages still under tests with no measurable room temperature condensation inside | 4 |
| Average lifetime to date (MTTF) including losses attributed to mishandling | 165 days |
| Average lifetime to date (MTTF) not including losses attributed to mishandling | 239 days |

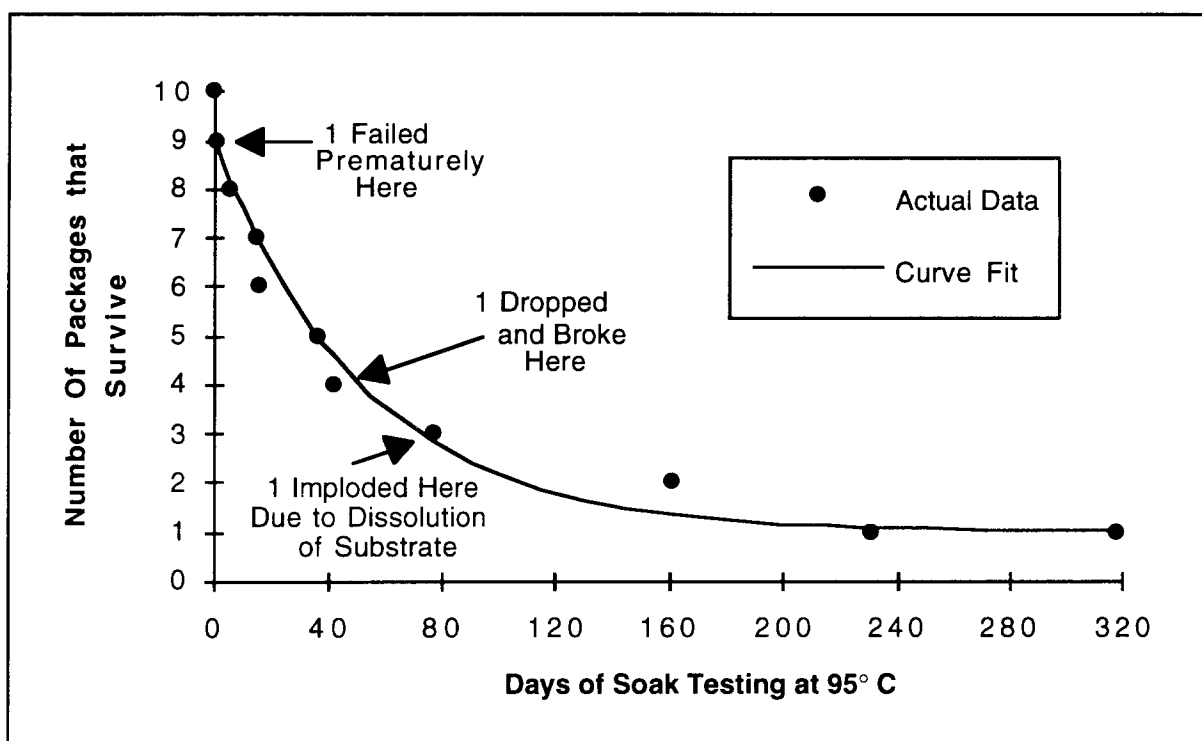


Figure 10: Summary of the lifetimes of the 10 packages which have been soaking at 95°C.

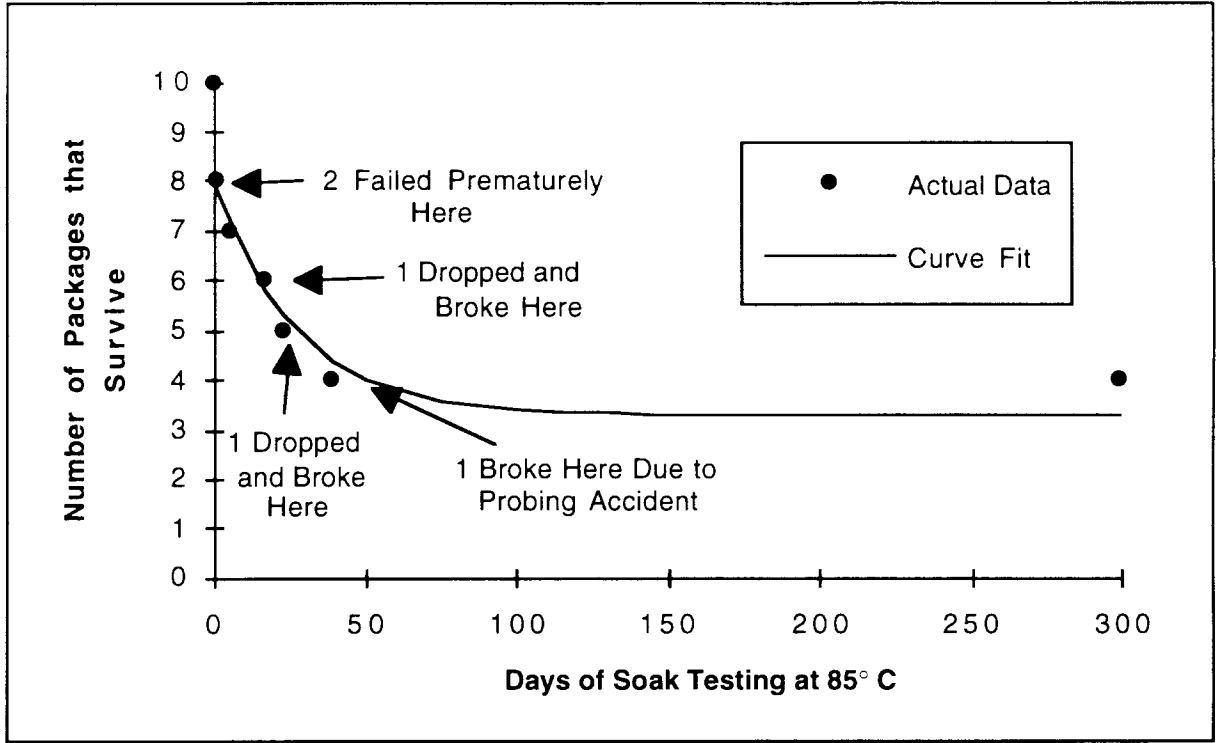


Figure 11: Summary of the lifetimes of the 10 packages which have been soaking at 85°C.

Assuming that leakage into the package is an Arrhenius process (such as diffusive leakage), it can be modeled with the following equation.

$$AF = \frac{MTTF_{Normal}}{MTTF_{Accelerated}} = e^{\frac{Q}{k} \left(\frac{1}{T_{Normal}} - \frac{1}{T_{Accelerated}} \right)}$$

Using the measured mean time to failure (MTTF) at 85°C and 95°C, the activation energy (Q) can easily be calculated, and from this the acceleration factor (AF) for these tests can be obtained, and then the MTTF at body temperature can be calculated. However we cannot accurately determine the activation energy in these tests yet because these are still ongoing. Until all of the samples show leakage, we cannot obtain MTTF at the accelerated temperatures. We can, however, obtain a worst case MTTF for the 85°C and 95°C soak tests by assuming that all remaining packages in these tests leak now. This worst case MTTF can be used to calculate the worst case activation energy, and hence the worst case MTTF at body temperature. Performing this calculation yields:

$$MTTF|_{85^{\circ}C} = 165 \text{ Days} \quad MTTF|_{95^{\circ}C} = 100 \text{ Days}$$

$$Q = 0.5687 \text{ eV}, AF(95^{\circ}C) = 29, AF(85^{\circ}C) = 17$$

$$MTTF|_{37^{\circ}C} = 7.8 Years$$

We call this average lifetime at body temperature of 7.8 years the worst case lifetime because every extra day that the remaining 85°C and 95°C packages last increases this projected lifetime. Also, it should be noted that we have included every single sample in the 85°C and 95°C soak tests in this calculation except the 15% which failed in the first day (we assume that these early failures can be screened for). However many of these capsules failed due to mishandling during testing, rather than due to actual leakage of the package. If we disregard the samples that we have attributed failure to mishandling, we obtain a somewhat longer mean time to failure:

$$MTTF|_{85^{\circ}C} = 239 Days \quad MTTF|_{95^{\circ}C} = 112 Days$$

$$Q=0.8608 \text{ eV}, AF(95^{\circ}C)=160, AF(85^{\circ}C)=75$$

$$MTTF|_{37^{\circ}C} = 49 Years$$

The above activation energy of 0.8608 is still somewhat lower than we expect for these packages. Again, this is because this activation energy is calculated using MTTF's at both temperatures if the tests were to fail today. In some smaller, preliminary tests on glass packages we obtained and reported an activation energy of 0.946. Using this activation energy, the corresponding body temperature mean time to failure for the packages in the 85°C and 95°C accelerated soak tests is:

$$Q=0.946 \text{ eV}, AF(95^{\circ}C)=256, AF(85^{\circ}C)=115$$

$$MTTF|_{37^{\circ}C} = 61 Years$$

The above calculations clearly indicate that the test data so far produces an expected mean time to failure of at least many years. As more data is collected and as these tests continue the above calculated figures are expected to only become larger. We will continue to report on the status of these tests, and we have also started tests on the new package that was reported in the previous section. The following summarizes the preliminary data that has been obtained from the new package designs so far.

2.1.4 Long Term Soak Tests On New Packages

During the past quarter we had started preliminary experiments using the new glass packages bonded to bare silicon wafers and observed that indeed very uniform and hermetic bonds can be achieved with the new capsules to full-wafer thickness substrates. This has been a very important result because so far we have been bonding the glass capsules to thinned silicon substrates, which made these substrates somewhat fragile. Since the new glass capsules have a much more polished and flatter bonding surface they can produce a good bond over the entire bonding region. In addition to these tests with bare silicon substrates, we also started tests with the latest set of package substrates that were completed this past quarter. We have bonded and started soak tests on 10 of these new glass-silicon packages. A photograph of one of these

packages is shown in Figure 12. The bonding parameters and temperature are the same as those used for the previous set of packages, and the bonds are very strong. Figure 13 shows an SEM view of one of the packages after the glass capsule has been broken away. As can be seen from this figure the bond is excellent over all the bonding region since we can see remnants of the glass capsule in all these areas. We have also started to soak these 10 packages in phosphate buffered saline at elevated temperatures. Of the original ten, three failed within the first day, which we have attributed to surface defects or improper alignment of the glass. This 30% rate of infant mortality is somewhat higher than our previously reported values which was 15%. We will increase the number of our soak tests and hope to obtain a statistically more reliable data set. However, one of the reasons for this relatively higher infant mortality rate could be that these new glass packages have been bonded to full thickness silicon substrates. During the coming quarter we are planning on thinning these silicon substrates and will attempt to isolate the problem and improve the yield. There are currently 7 packages that are soaking at 85°C in saline: one soaking for 13 days, one for 9 days, three for 7 days and two for 6 days. We will continue these tests, and will start more packages at 37°C, 85°C, and 95°C, all in phosphate buffered saline solutions. As mentioned in previous reports we have observed dissolution of silicon in saline at higher temperatures. To overcome this problem, the saline solution of the ten new samples has been changed daily to keep the concentration of the solution constant. This procedure has so far resulted in cleaner looking glass capsules and will probably resolve the dissolution problem.

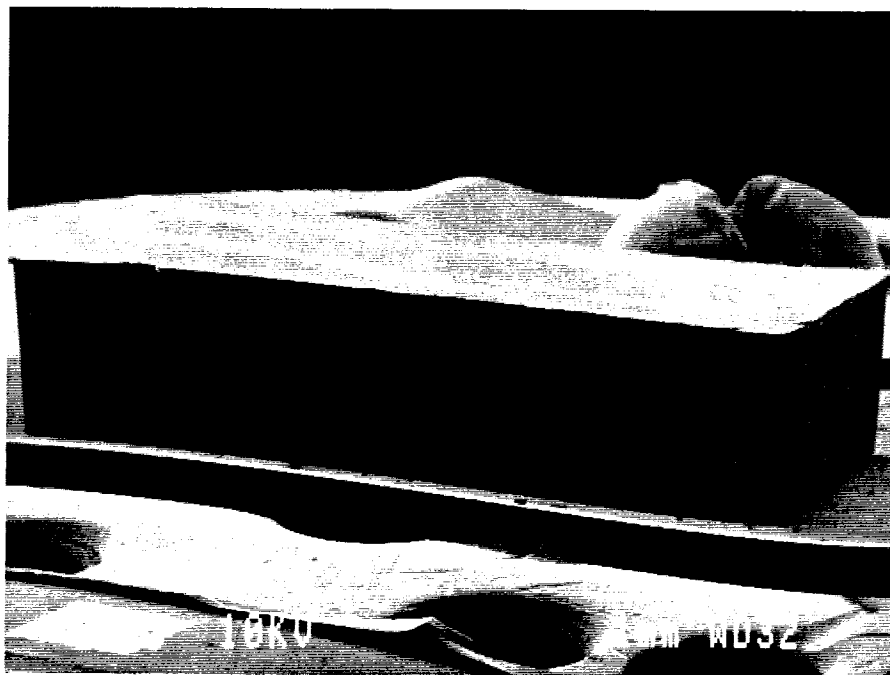


Figure 12: SEM photograph of a new glass capsule bonded to a silicon package substrate.

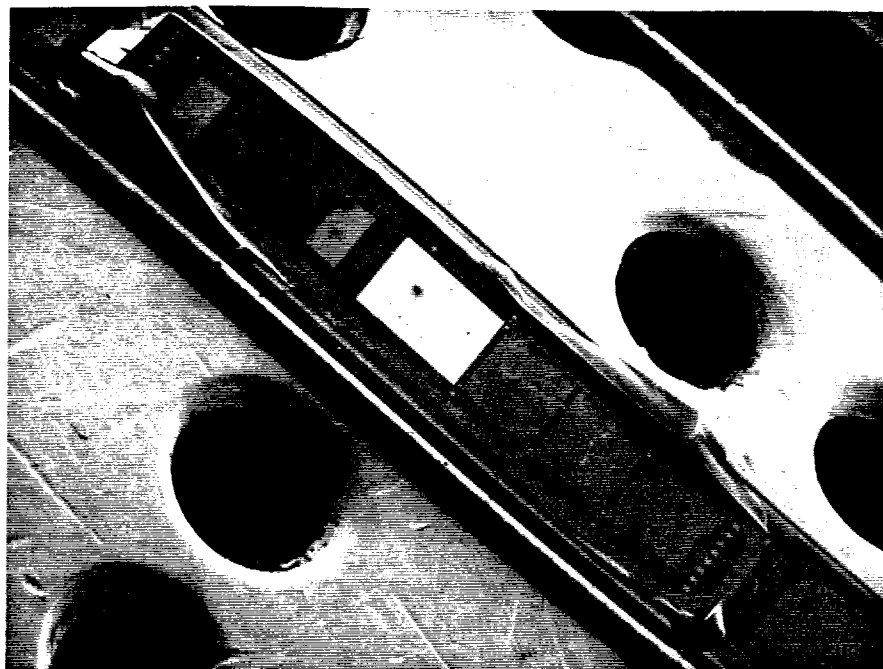


Figure 13: SEM view of the bonding region of a package after it is manually broken apart from the silicon substrate.

2.1.5 Ongoing Room Temperature Soak Tests

For over 7 months we have been soaking a group of packages in phosphate buffered saline at room temperature. These tests have enabled us to both obtain test results in saline solutions (as opposed to tests in DI water used for the other packages under test), and to obtain some soak test data independent of the acceleration technique used. Admittedly, the room temperature tests will take a long time to produce meaningful data. However, the results obtained this way will act as a good control to verify the overall integrity of the package.

We started soaking six packages in saline at room temperature. One of these packages leaked within a day, indicating surface defects or poor alignment of the glass capsule to the silicon substrate. All five of the remaining packages show no sign of moisture either measured electrically or observed visually. Three of these five packages have been soaking now for 222 days, a fourth has been soaking for 188 days, and the fifth for 176 days. Table 4 summarizes these room temperature soak tests.

Table 4: Data for room temperature saline soak tests in saline.

| | |
|--|----------|
| Number of packages in this study | 6 |
| Failed within 24 hours (not included in MTTF) | 1 |
| Longest lasting packages so far in this study | 222 days |
| Packages still under tests with no measurable room temperature condensation inside | 5 |
| Average lifetime to date (MTTF) | 206 days |

2.1.6 Characterization of High Temperature Capacitors:

We have been searching for a hybrid chip capacitor that could withstand the high bonding temperature required for the anodic bonding process. The requirement for these capacitors is that they should be sufficiently small to fit into the glass package and still have a relatively high capacitance value. It is also required that they maintain their electrical properties after being exposed to the high temperature cycle at 340°C for 10 minutes. We have finally found a company that makes multi layer chip capacitors which could withstand the higher bonding temperatures. It should be noted that two years ago we had located another vendor that fabricated tantalum chip capacitors, which also were capable of withstanding bonding temperatures of about 320°C. However, our experience during the past two years with these capacitors revealed that some of them failed at bonding temperatures below 320°C. In addition, the vendor that made these capacitors does not fabricate them any longer. The new company routinely produces the new capacitors, and we feel that we are in very good shape in terms of the temperature resistance of all the hybrid components. After obtaining a sample set of 25 capacitors, we have subjected them to temperature tests, whose results are detailed below.

The initial tests were performed using a small set of 5 capacitors. The dimensions of these capacitors are 3.18mm (length), 1.52mm (width) and 1.52mm (height). These capacitors were first measured carefully with a compensated gain phase analyzer from 100 Hz to 40 kHz. After this measurement, the capacitors were heated on a silicon packaging substrate placed on a hot plate inside the cleanroom precisely mimicking a routine packaging process. To be more precise, the Pyrex container used during an actual bonding procedure was utilized to sustain a uniform temperature around these sample capacitors. During this test, the capacitors were exposed to a heat cycle of 340°C for about 10 minutes and then the hot plate was turned off allowing the capacitors to cool down to room temperature slowly.

After this heat cycle the capacitors were measured carefully with the compensated gain phase analyzer. Figures 14 and 15 show the capacitance and equivalent series resistance values before and after the heat treatment. Comparing both sets of measurements, we observe that there is a minor increase in the value of the capacitance and a slight decrease in the value of the equivalent series resistance; the changes being less than 5% of the total values. In summary, the electrical characteristics of the samples did not change appreciably due to this heat cycle. There was no observable change in the physical appearance of these samples; as opposed to some of the previous samples that either swelled, or changed color, or even exploded in some cases. We are confident that these capacitors will be very appropriate for our packaging applications that incorporate hybrid components.

After performing the tests at 340°C, we also performed a set of heat cycling experiments at 400°C using 2 capacitors. These measurements are also done by placing the samples on silicon substrates and then placing them on a hot plate heated up to 400°C inside the cleanroom. Figures 16 and 17 show the capacitance and equivalent series resistance values before and after the heat treatment. Similar to the situation above, the capacitors preserved their physical and electrical characteristics. We are very enthusiastic about these capacitors and have already begun preliminary assembly experiments using these capacitors which would be detailed in the later sections of this report and also in the next report.

Comparison of capacitance after 340C, 10 mins

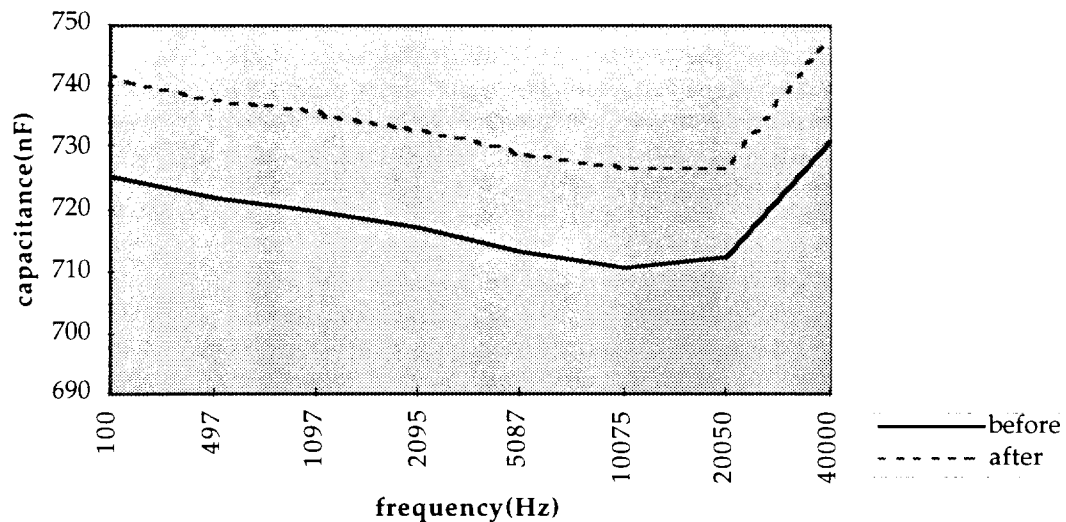


Figure 14: The effect of the heat cycle on the new chip capacitors. The dotted line shows the values of the capacitance after the heat cycle(340C, 10 minutes), whereas the solid line is the value of the same capacitance before the heat cycle.

Comparison of resistance after 340C, 10 mins

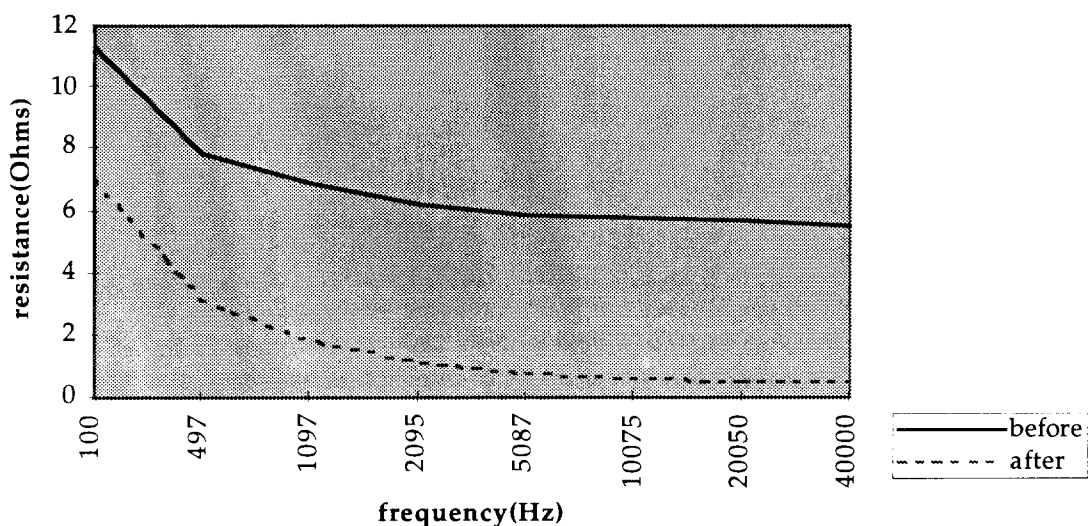


Figure 15: The effect of the heat cycle on the new chip capacitors. The dotted line shows the values of the equivalent series resistance of the capacitors after the heat cycle(340C, 10 minutes) whereas the solid line is the same parameter before the heat cycle.

Comparison of capacitance after 400C, 10 mins

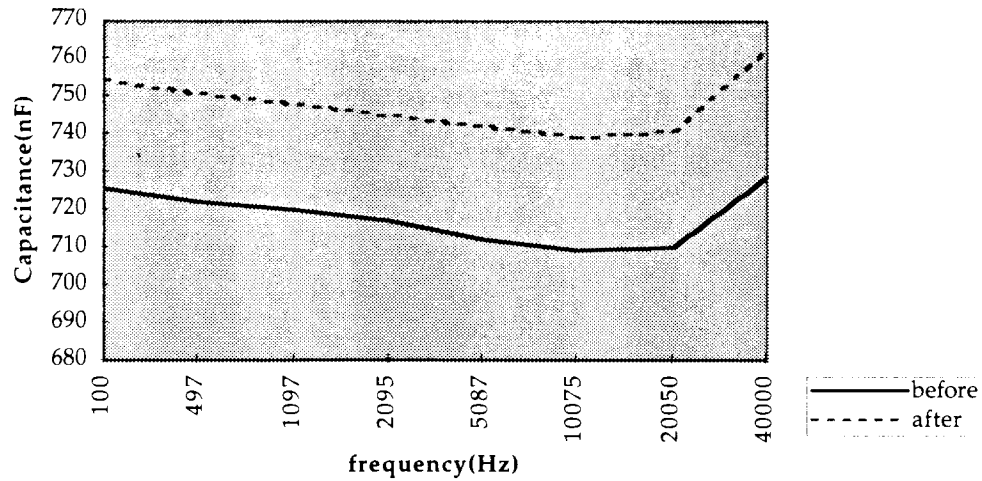


Figure 16: The effect of the heat cycle on the new chip capacitors. The dotted line shows the values of the capacitance after the heat cycle (400C, 10 minutes), whereas the solid line is the same value of the capacitance before the heat cycle.

Comparison of resistance after 400C, 10 mins

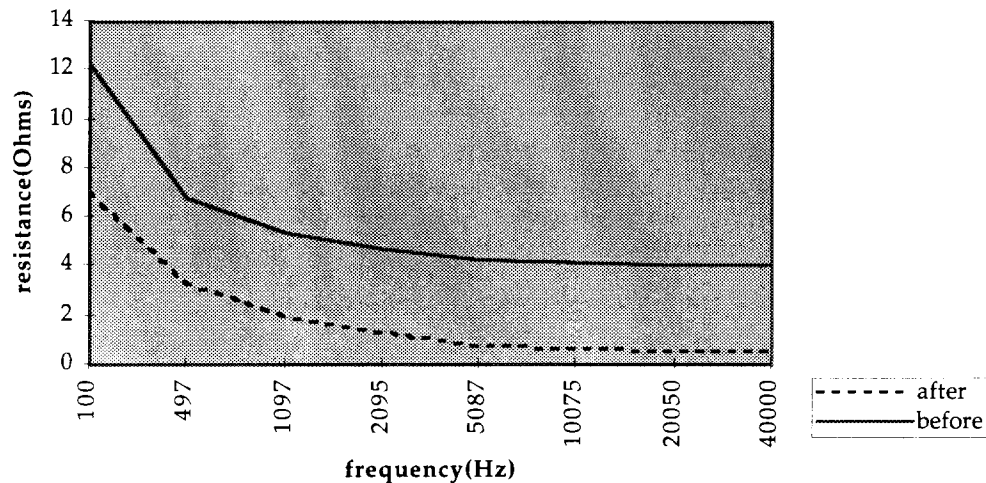


Figure 17: The effect of the heat cycle on the new chip capacitors. The dotted line shows the values of the equivalent series resistance of the capacitors after the heat cycle (400°C, 10 minutes) whereas the solid line is the same parameter before the heat cycle.

2.1.7 In-Vivo Tests

In the last progress report we presented preliminary data on in-vivo tests performed on glass-silicon packages implanted on the dura of guinea pigs. Those tests did not reveal any adverse reaction in the tissue. During the last quarter we sent 5 packaged substrates with no microstimulator circuitry inside to Vanderbilt University to be implanted into rats. These packages used the old glass capsules, and the silicon package substrates containing all the materials needed in obtaining a good hermetic package. Therefore, except for the functionality of the devices, they were an exact mockup that could be successfully used for animal studies. Our colleagues at Vanderbilt implanted these packages and have performed histology studies on them as reported below.

Animal Studies Conducted through Consortium with Vanderbilt University

The overall goals of the consortium studies are to design a microstimulation device appropriate for reanimation of paralyzed PCA muscles (the openers of the voice box), and to assess the biocompatibility, positional stability and functional status of such a device. Reanimation of these muscles with an injectable microstimulator in a patient with paralysis could provide a nonsurgical method of rehabilitation, restore the airway to a patient, and prevent asphyxiation.

Specific aims this first year have been to determine the general configuration and dimensions of a microstimulator in acute canine studies and to assess the biocompatibility of a prototype device in chronic implantation studies on the rat. After considerable design modification, five prototype devices deemed appropriate for laryngeal implantation were delivered to Vanderbilt for biocompatibility studies. Under halothane anesthesia, incisions were made in the dorsum of each rat. In two rats, a device was implanted paraxially to the vertebral column in a subcutaneous pocket overlying the latissimus dorsi or trapezius muscles. In the remaining rats, additional materials were implanted under separate incision as controls. The materials included type 316 stainless steel wire, Teflon sheet, and Silastic tubing (Dow Corning). After 1 month, the device and surrounding tissue were harvested from the first two rats. As shown in the photograph in Figure 18, there was no evidence of tissue inflammation, edema, or infection indicative of microstimulator (MS) rejection macroscopically. At a microscopic level, hematoxylin-eosin stained tissue in direct apposition to the implanted device appeared normal and showed no sign of rejection (Figure 19). There was no evidence of edema or inflammatory reaction as suggested by macrophage or polymorphonucleocyte (PMN) infiltration of any tissue component including epidermis (E), hair follicle (HF), muscle (M), or connective tissue (CT).

For the remaining quarter of this year, the biocompatibility studies will continue through harvest and analysis of tissue and devices from remaining rats and further chronic implantation studies. In addition, the acute canine studies will be performed as originally planned to evaluate device configuration.



Figure 18: Photograph showing the tissue quality after one month of implantation of the microstimulator package.

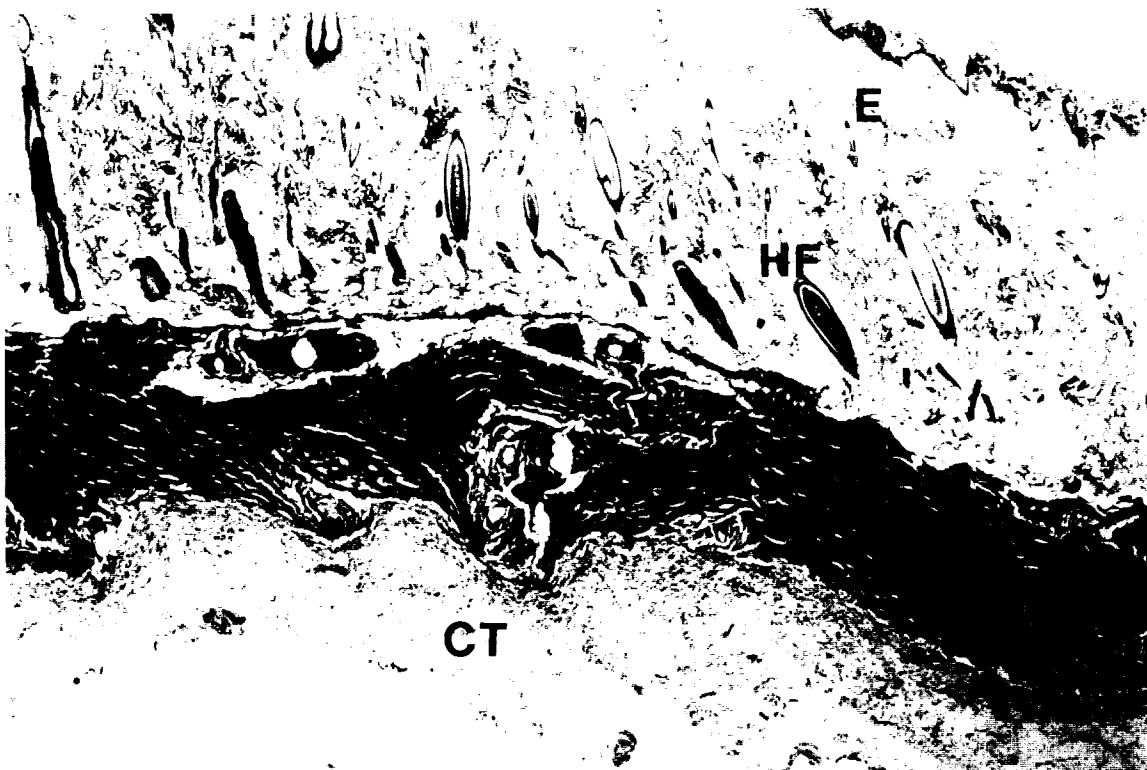


Figure 19: Hematoxylin-eosin stained tissue in direct opposition to the implanted microstimulator device appears normal with no sign of rejection.

2.2 Microstimulator Testing And Assembly

In the past quarter, we finished a new fabrication run of Microstimulator chips and began testing and packaging these chips. We have succeeded in packaging the first complete, working Microstimulator and have gained substantial experience toward reliably producing more such units in the coming quarter. We have previously presented detailed results on microstimulator circuit testing. Therefore, in the following we will not discuss circuit testing, rather we will concentrate on the issues faced in assembly and operation of the completely packaged microstimulators.

The new wafers are passivated with a top layer of protective, insulating low-temperature silicon dioxide so that the circuitry will not be harmed when handling and packaging the chips. Openings have been etched in the oxide where contact to the metal pads is necessary. Copper is electroplated in the openings to a thickness of about 10-15 μ m, to form not only on-chip coils for the bidirectional microstimulator, but also thick pads over which the microcoils can be microwelded. Stimulation charge storage capacitors will also be attached with conductive epoxy directly to their respective pads.

Copper has been selected instead of nickel (used in the previous quarter) because of its lower resistivity. Additionally, we have developed a well-defined and predictable copper electroplating process. The resulting electroplated copper film is of very good quality, although it is somewhat granular. The granularity of the film thus far has posed no problem when microwelding the copper wire microcoils to the copper pads. With considerable force the wire leads can be torn from the copper electroplated surface, possibly because the granular surface provides slightly less contact area for the lead. Nonetheless, the microwelding force can easily be increased to compensate for this, pressing the leads more strongly onto the pads. It should be noted also that the copper to copper microwelds have been found to have very negligible resistance. Typically we have measured about 0.2 Ω of contact resistance per microweld.

2.2.1 Telemetric Functionality Testing Of New Microstimulator Batch

We have been systematically testing the Microstimulator dice from the current fabrication run using our probe station, operating them through a telemetric link. The link utilizes a prototype portable transmitter unit. The link is very highly coupled in this case, using a small (roughly 1cm diameter) transmitter coil and a microcoil (roughly 4mm[leng.]x1.5mm[diam.]) connected to the Microstimulator through coaxial cables. We have described such a setup in previous reports. This highly coupled setup is necessary because of the parasitic detuning resulting from the coaxial cables and probing equipment. Also, we do not wish to immediately cut tuning capacitors on chip merely for tuning when testing, since this will not provide us with sufficient flexibility when it becomes necessary to tune each Microstimulator individually before it is assembled and shipped. The strong link allows us to receive more than adequate power when testing, despite the relatively low Q of the transmitter when using this small transmitter coil. The transmitter coil, though physically small in this case, has a substantial series resistance which reduces the overall Q of the transmitter.

Some cuts, however, must be made on each chip before it is tested. Each Microstimulator has been designed to respond to a five bit digitally encoded address. All units respond to the code "11111" and can respond to one of thirty-one other unique addresses (thirty-two in all). This individual address is chosen and cut with the laser before the chip is tested. Two other cuts help to determine the amount of time that the received signal must remain high during any given bit period to distinguish a digital "one" from a digital "zero." These cuts can not be ignored, since doing so does not leave the bits at a default value but instead permits a short between the 4V on chip supply and ground reference; when the bits are programmed they

are left connected to either the 4V supply or ground. Nonetheless, these seven cuts do not add substantially to the preparation time required for each chip, and the laser cuts can be made successfully and consistently cleanly.

When testing the DC input characteristics of the Microstimulators to ensure that the above cuts had been made cleanly, it was noted that certain dice, especially those closest to the edges of the wafer, drew less current than expected, about 2-2.5mA versus 2.9-4mA. The problem is particularly aggravated, as indicated, toward the edges of the wafers. This tendency of the CMOS logic circuitry not to work well on dice close to the edge of the wafer was confirmed in many dice. Thus the current yield is not as high as it potentially can be, relying primarily on good dice close to the center of the wafer. We have other wafers left that we have not yet finished processing but that we expect to finish soon. Overall yield from those wafers can be expected to be much better. In the meantime, we have gotten several working dice from the current wafers.

Among the corrections made in the current batch of Microstimulators is a considerably more robust and reliable envelope detector. Although the design is adjustable to a great extent, thus far it has worked without modification on virtually all of the Microstimulator chips tested. The envelope detector has been noted to work reliably with bit rates of up to 83 kHz (five bits in 60 microseconds). The power-on-reset (POR) feature has been corrected, with the new metal mask incorporating by default the most reliable of the three POR designs included on the Microstimulator chip.

The clock has been shown to work virtually unfailingly. In addition, the logic and output circuitry have again been demonstrated to work fine.

We are still examining one functional feature of the chip that has proved difficult to confirm, namely the individually addressed control mode. From the current wafers, we have only sporadically succeeded in causing individual Microstimulator chips to respond to their own unique addresses. All of the otherwise working chips have been able to respond to the "11111" default code, however, and this capability gives us units for immediate use. We believe that we will decipher this individual addressing problem soon. The problem may be related to the our low yield, and thus may be corrected on the next wafers that we finish in the near future.

2.2.2 Assembly

We made progress in the past quarter in preparing a workable packaging and assembly strategy for the complete Microstimulator. We anticipated many of the problems that were likely to arise in assembly and then carried out assembly tests to gain experience before risking actual working chips. Recent experiments have given us so much data and preliminary experience that we feel confident that soon (i.e. early in the coming quarter) we will be able to package complete working systems with considerably greater reliability and ease than at first. Table 5 summarizes the current assembly strategy.

A number of steps have now been developed that will further facilitate the assembly process. First, the microcoil must be welded onto the chip first, before the stimulus charge storage capacitor is mounted. This is simply because the microwelding machine's weld head actually touches the capacitor when trying to weld to one of the coil's pads if the capacitor is already in place. The microweld joints are further strengthened by covering them with either epoxy or high temperature polyimide. In some of our early tests we have used non-conductive epoxy to insulate the microweld joints, and attach the coil to the circuit chip. This nonconductive epoxy can also be used to passivate exposed areas of the chip underneath and adjacent to the capacitor, especially close to the capacitor attachment pads.

Table 5: Assembly Procedure For Microstimulator

I. CHIP LEVEL PREPARATION

- A. Electroplate copper on titanium / copper plating base.
- B. Thin wafer if necessary, for clearance and for ease of wire bonding.
- C. Dice wafer.
- D. Microweld receiver coil on chip.
- E. Passivate critical areas, reinforce leads.
- F. Attach capacitor on chip with conductive epoxy; cure epoxy.
- G. Test to confirm adequate connection of coil / capacitor.

II. FIRST CLEAN ROOM PHASE

- A. Clean packaging substrates.
- B. IPA rinse / DI water rinse / dry circuit.
- C. Glue chip to packaging substrate (nonconductive epoxy).

III. WIRE BONDING

Four connections: logic output, 2 electrodes, 1 redundant to capacitor.

IV. SECOND CLEAN ROOM PHASE

- A. IPA / DI water clean circuit mounted on packaging substrate.
- B. Dehydration bake @ 150°C / 2 hours or other recipe.
- C. Anodic bond glass capsule.
 - 1. Thoroughly preheat chips to complete outgassing before anodic bonding.
 - 2. Clean capsules thoroughly, ahead of time.
 - 3. Align cold / ramp up temperature.
- D. Cool samples and store in sealed Teflon containers.

V. PRE-SHIPPING PHASE

- A. Prepare for activation.
 - 1. Telemetric functionality test.
 - 2. Attach to PC stalks for activation.
 - 3. Store until activation / shipping time.
- B. Activate.
 - 1. If activated here, need to use in-house activation station.
 - 2. Must store / ship in solution after activation.
 - 3. Optionally, could let user activate if capable.
- C. Perform final mechanical preparations: scribe end pad section off.

VI. SHIPMENT: Once activated, must be in solution for all but very brief times.

2.2.3 Anodic Bonding With Circuitry And Hybrid Components Encapsulated

As a preliminary step to packaging a complete Microstimulator, we first performed tests to examine the effect of having actual circuits with hybrid components inside the package when bonding. We experimented with a microwelded coil on the chip and with capacitors as well. Primary objectives of these tests were to examine whether we have adequate clearance within the capsule or whether we must thin the circuit dice; whether sparking occurs to the hybrid components or chip, and if that sparking is destructive; and whether the glass to silicon bond is still reasonably strong despite the presence of substantially large objects within the packages (and the resulting difficulty in position of the glass, etc.). The packages were opened shortly after bonding, so we did not collect data on hermeticity from these experiments.

In the case of the coil microwelded on a nonworking Microstimulator chip (Figure 20), we observed a significant, relatively high peak in the bonding current during the first minute of the bond. The air within the capsule could actually be seen to have a purple glow with occasional sparking to the coil which was evidently very close to the sides and top of the glass package. This glow eventually subsided. Actually, after breaking the capsule open, it could be seen that the coil must have been touching the top and at least one side of the glass package. At sufficiently high magnification, the polyimide insulation used to set the coils after they are wound and perhaps some of the nonconductive epoxy used to glue the coil in place to the chip can clearly be seen to be greatly darkened throughout and somewhat flattened where the coil touched the glass. Additionally, the inside of the capsule can be seen to have a brown residue. It can be presumed that this residue resulted from outgassing from the coil. It was speculated in the previous report that the darkening of the coils when heated was accompanied by outgassing and that it would be best to preheat the coils at the bonding temperature for an extended amount of time before encapsulation. This step was omitted in the case of this coil, and we observed the resulting brown residue.

It was noted that a dark, sooty deposit formed on all of the electroplated pads, even extending slightly beyond individual pads to the spaces between them. It is possible that this material is being deposited during the period of time in which the purple glow is observed within the capsule, and that it is chemically composed of residues being vaporized from the surface of the coil and from the non-conductive epoxy. This epoxy cannot withstand the high bonding temperatures and will not be used in the future. We plan on using polyimide for insulating and attaching the coil to the chip. Polyimide can withstand temperatures as high as 400°C, which is certainly compatible with the bonding temperature. The deposit is a thin, crusty material that can be removed in flakes with a probe tip. It does not seem to be mere oxide, since when the material is removed, the surface below appears to be the original, granular electroplated copper layer. Also, an oxide might be expected to be confined more precisely to the pads. A SEM picture of this sooty deposit is included as Figure 21, in this case the pads of a chip with a capacitor bonded. The material may be carbon since we do observe a much smaller resistance between the bonding pads than on clean chips.

The coil's electrical properties did not suffer despite the sparking inside the capsule. The on chip tuning capacitors were disconnected from the coil, so that the coil alone could be studied through its bonding pads. The inductance remained essentially the same as before being subjected to electrostatic bonding, and the heat did not harm the polyimide insulation.

Capacitors bonded on chips and then electrostatically encapsulated behave in a similar way. Again a purple glow is seen in the initial phase of the electrostatic bonding, accompanied by sparking and a brief, relatively high current. The glass package shows some darkening closest to the capacitor, but the capacitor does not outgas to the same extent as a coil that has not been extensively preheated. The ceramic capacitor itself darkens very slightly in color but does not

show signs of burn damage. When measured after removing the glass capsule, the capacitance remains essentially the same as before anodic bonding, about $0.7\mu\text{F}$.

Although these packages were not intended for hermeticity tests, it can be seen from Figure 22 that the glass to silicon bond is quite strong despite the relative difficulty of properly placing the glass over the substrate when a microchip and hybrid components are contained inside the package. Remnants of glass on the silicon packaging substrate offer evidence of the strength of the anodic bonds achieved in these cases.

We are very encouraged by the results obtained from these tests, since we believe we can improve the cleanliness inside the package to a great extent, which will help the bonding quality even further. Even under the non-optimum conditions of our preliminary tests we have been able to get good electrostatic bonds using the new glass capsules. In the coming quarter we will assemble our good circuit chips and will start testing some of the fully assembled units for both hermeticity and telemetry operation.

2.3 Microstimulator Circuit Fabrication

In the past quarter we completed testing of the microstimulator circuitry and verified its functionality. After completion of this testing we proceeded with the final step in the fabrication of both the single and multi-channel microstimulator circuit chips, passivation of the circuitry and definition of the second layer electroplated metal. The circuit passivation is required in order to protect the metal interconnect from being shorted or otherwise disturbed during the final assembly and packaging of the microstimulator.

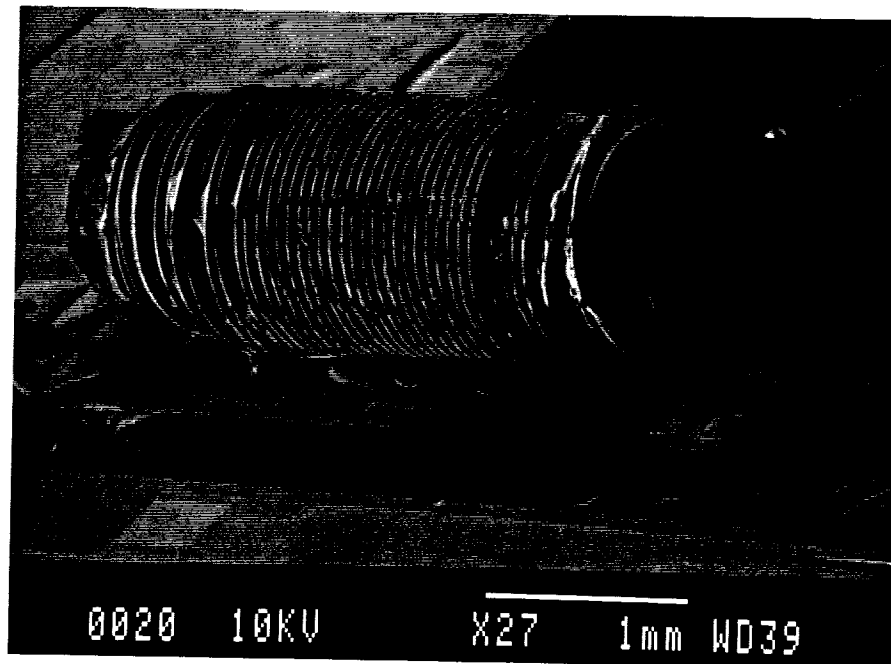


Figure 20: This coil, microwelded to a Microstimulator chip, is shown after surviving anodic bonding inside a glass capsule.

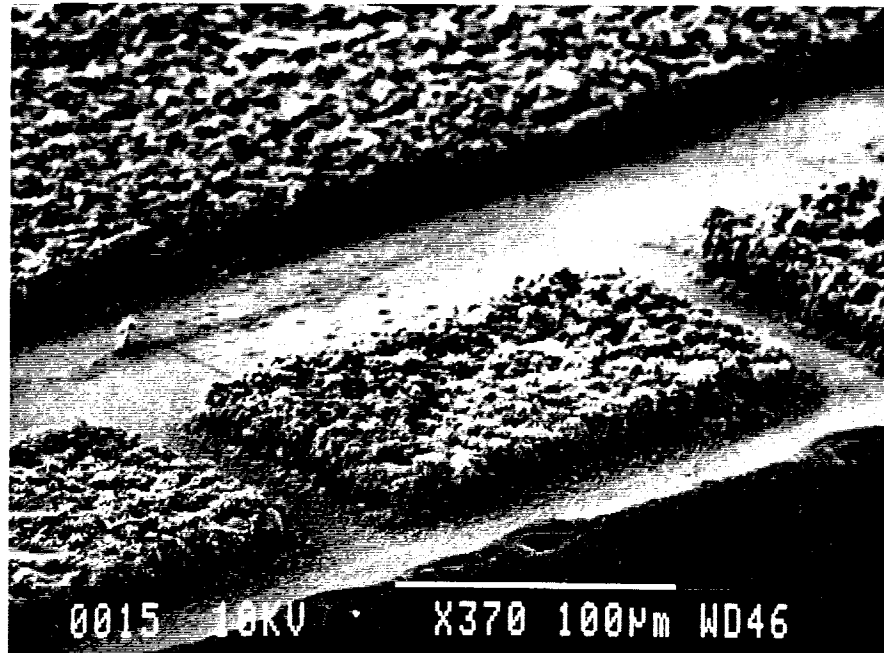


Figure 21: A dark deposit can be plainly seen on the exposed pads of a Microstimulator chip after anodic bonding with hybrid components inside the glass package.

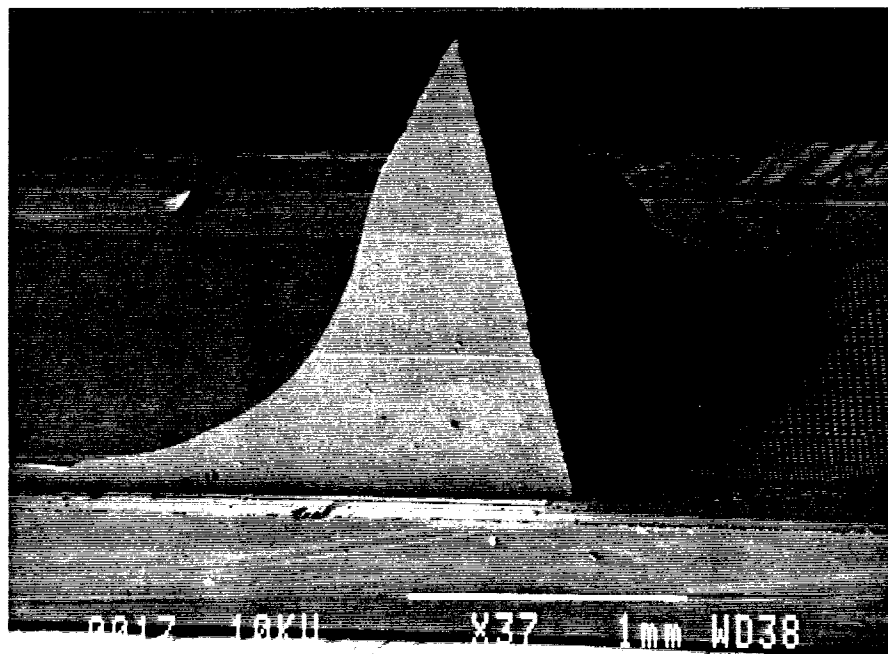


Figure 22: View of the broken corner of a glass capsule that was anodically bonded to this packaging substrate. The package contained a Microstimulator chip with ceramic capacitor bonded to the chip.

A second layer metal is required to be electroplated on chip for two reasons. The first reason is that a microwelder is to be used for connecting the hybrid power reception coil to the microstimulator circuit. The microwelder utilizes a high level of electrical current flow in order to get a good bond between the wire of the hybrid coil and the bonding pads, and this can destroy thin metal pads that are sputtered or evaporated on-chip. The metal bonding pads are fabricated using electroplated metal $>10\mu\text{m}$ thick, so that they can withstand the microwelding procedure. The second reason for using an electroplated second layer metal is to provide a high quality coil for the active on-chip transmitter of the multi channel microstimulator.

The final fabrication consists of the following steps, as is shown in Figure 23. First, the passivation is provided by a $2\mu\text{m}$ thick LTO layer that is deposited by LPCVD at 420°C . The LTO is patterned with via holes in order to provide places for the metal2 layer to contact the metal1 layer. Next, a Cr/Cu metal layer is deposited over the entire wafer which acts as an electroplating base for the second layer metal. A mold is now made from a $19\mu\text{m}$ thick photoresist for electroplating the metal2 layer. The final process used for creating this photoresist mold is not very complex, however, several weeks were spent in determining the optimal spin speeds, softbake time, exposure time, development formula, and other procedures necessary when using thick photoresists. After creating the photoresist mold, a $12\mu\text{m}$ thick copper layer is electroplated on the wafer. The photoresist mold is then removed, and lastly, the Cr/Cu electroplating base is removed in the areas that were not electroplated with the metal2 layer. These final steps also required 2-3 weeks to determine a reliable fabrication procedure, but they have been completed and Figure 24 shows two SEM photographs of an electroplated copper coil on a fabricated multichannel microstimulator circuit chip. We have just begun testing of the microstimulator circuitry with the electroplated metal2 layer, and have achieved good results so far. Of particular interest is the quality of the signal that can be received from the on chip active transmitter and coil for the multichannel microstimulator. These tests are just being started and will be included in the next quarterly report.

3. PLANS FOR THE COMING QUARTER:

Our activities for the coming quarter will proceed in several areas. First, we plan on continuing soak testing of the old glass packages and start a large number of tests using the new glass packages. We now have the silicon substrates needed to do this and have developed the bonding procedure for the new capsules. In-vivo animal tests will also continue both here at Michigan and at Vanderbilt. We will provide additional packages to our colleagues at Vanderbilt for additional implants in rats.

Second, the assembly procedures and packaging of the complete microstimulators are now in place and we will have a number of complete devices ready for testing. We plan on fabricating a sufficient number of packaged samples that we can start soak testing to verify the integrity of the package with all the components inside.

Finally, we will also continue testing of the multichannel microstimulator chips, which have been waiting for the copper electroplating step, which is now complete. We will report on the result of this microstimulator in the next progress report.

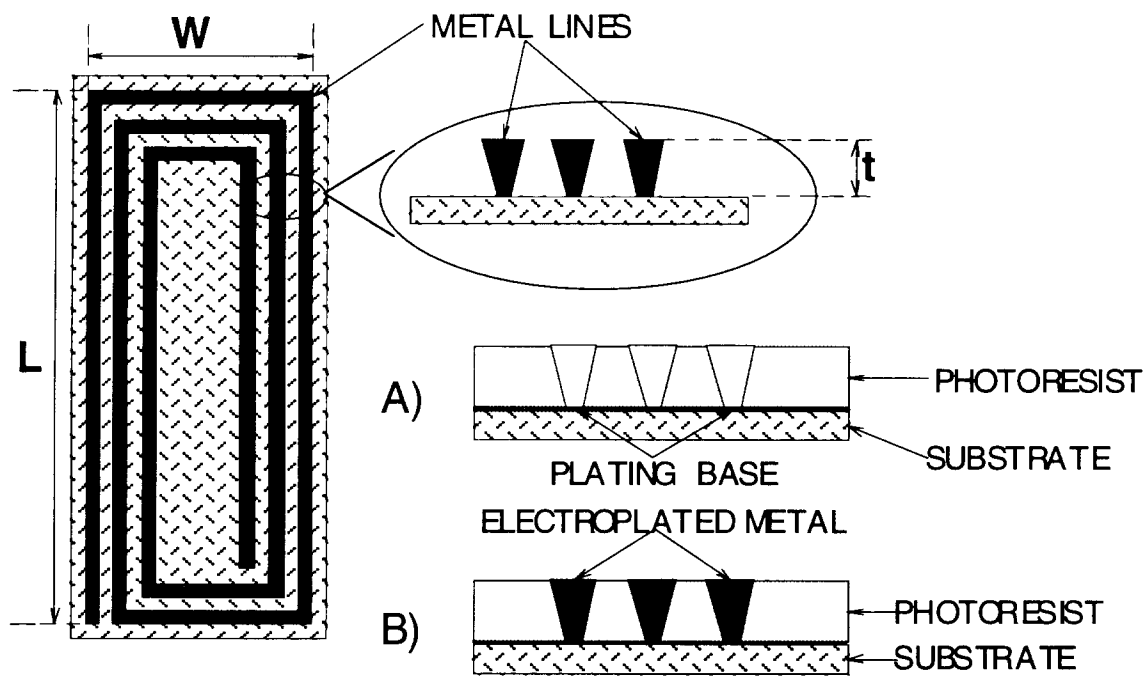


Figure 23: Fabrication process for a thick electroplated second layer metal.

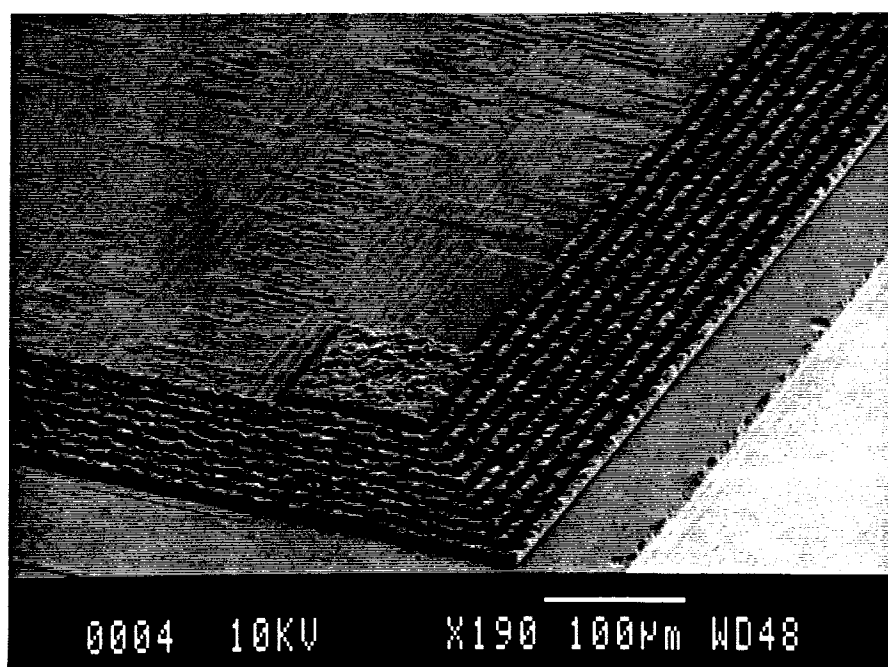
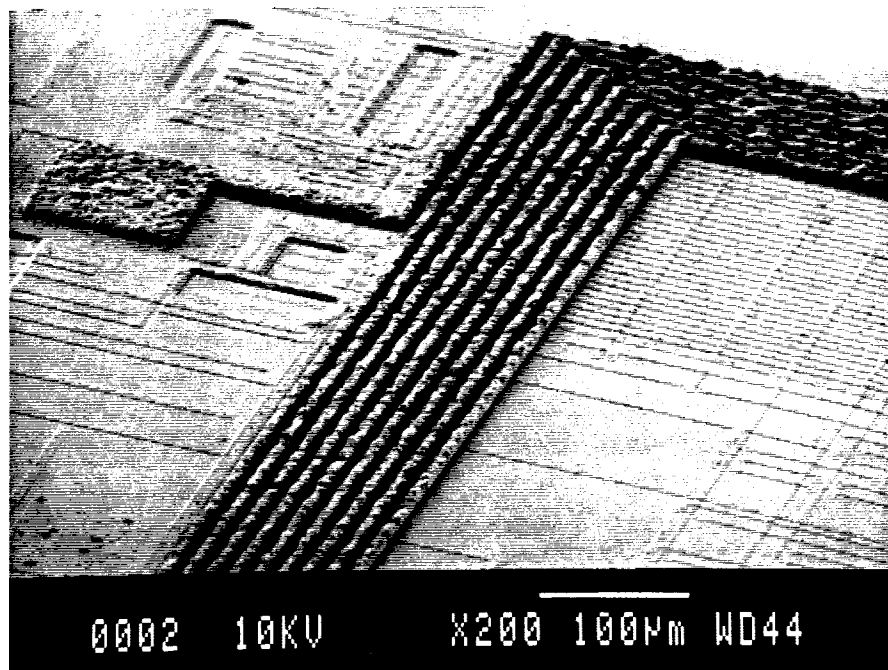


Figure 24: Two SEM photographs of an electroplated copper coil on a fabricated multichannel microstimulator circuit chip.